

**Liquid-phase Thermodynamic Properties of New Refrigerants,
Pentafluoroethyl Methyl Ether and Heptafluoropropyl Methyl Ether¹**

Hirofumi Ohta², Yoshiyuki Morimoto^{2, 4}, Januarius V. Widiatmo^{2, 3}

and Koichi Watanabe^{2, 3}

¹Paper presented at the Fourteenth Symposium on Thermophysical Properties, June 25-30, 2000, Boulder, Colorado, U.S.A.

²Department of System Design Engineering, Faculty of Science and Technology, Keio University, 3-14-1, Hiyoshi, Kohoku-ku, Yokohama 223-8522, Japan

³Permanent Researcher at Agency for the Assessment and Application of Technology, J1. M. H. Thamrin No. 8, Jakarta 10340, Indonesia

⁴To whom correspondence should be addressed.

Abstract

In the present paper, we report an experimental study on the liquid-phase thermodynamic properties of the new-generation alternative refrigerants, pentafluoroethyl methyl ether, $\text{CF}_3\text{CF}_2\text{OCH}_3$ (245cbE $\beta\gamma$), and heptafluoropropyl methyl ether, $\text{CF}_3\text{CF}_2\text{CF}_2\text{OCH}_3$ (347sE $\gamma\delta$). The measurements of vapor-pressures, saturated- and compressed-liquid densities were performed by means of a magnetic densimeter coupled with a variable volume cell mounted with a metallic bellows for temperatures from 260 to 370 K (for $\text{CF}_3\text{CF}_2\text{OCH}_3$), 250 to 370 K (for $\text{CF}_3\text{CF}_2\text{CF}_2\text{OCH}_3$) and pressures up to 3 MPa. The experimental uncertainties of the temperature, pressure and density measurements were estimated to be within ± 8 mK, ± 2 kPa and ± 2.2 kg·m⁻³, respectively. The purities of the samples used throughout the measurements were 99.99 mass% for $\text{CF}_3\text{CF}_2\text{CF}_2\text{OCH}_3$ and 99.9 mass% for $\text{CF}_3\text{CF}_2\text{OCH}_3$. Based on these measurements and the available data reported by other investigators, the thermodynamic behaviors with respect to vapor pressures, saturated- and compressed-liquid densities are discussed in terms of vapor pressure and saturated liquid density correlations developed and a liquid-phase equation of state. By examining the thermodynamic behavior of the derived properties such as the specific isochoric and isobaric heat capacities, speeds of sound and Joule-Thomson coefficients, the range of validity for the developed models and their physical soundness will be discussed.

Key Words: compressed liquid density, equation of state, fluorinated ether, heptafluoropropyl methyl ether, new-generation refrigerant, pentafluoroethyl methyl ether, $P\rho T$ properties, saturated liquid density, thermodynamic properties, vapor pressure

Introduction

In accord with the increasing concerns about the global warming impact by released hydrofluorocarbon (HFC) refrigerants, several hydrofluoroether (HFE) refrigerants recently developed are considered as promising long-term replacement to some HFCs. HFE refrigerants, pentafluoroethyl methyl ether, $\text{CF}_3\text{CF}_2\text{OCH}_3$ (245cbE $\beta\gamma$), and heptafluoropropyl methyl ether, $\text{CF}_3\text{CF}_2\text{CF}_2\text{OCH}_3$ (347sE $\gamma\delta$), have vapor-pressures similar to those of dichlorotetrafluoroethane (R-114) and trichlorofluoromethane (R-11), respectively. These HFE refrigerants have lower global warming potential than R-114 and R-11, respectively. So they are expected as a promising alternative to replace R-114 and R-11. The present study, therefore, aims to investigate the vapor-pressures, the saturated- and compressed-liquid densities of $\text{CF}_3\text{CF}_2\text{OCH}_3$ and $\text{CF}_3\text{CF}_2\text{CF}_2\text{OCH}_3$.

Experimental

All experimental measurements in the present work were performed with a magnetic densimeter coupled with a variable volume cell, which enabled measurements either at the saturated-liquid or at the compressed-liquid condition. The experimental apparatus is shown in Figure 1. The magnetic densimeter (A) consists of a buoy equipped with a permanent magnet, a sample cell, an electromagnetic coil and a search coil. The sample density was measured by the magnetic densimeter immersed in a thermostated fluid bath (E). The sample pressure was directly measured by a digital quartz pressure transducer (C) with the aid of a digital quartz pressure gauge (F) and a digital quartz pressure computer (J). The temperature was measured by means of a standard platinum resistance thermometer (R) placed in the vicinity of the magnetic

densimeter. By controlling the pressure of the nitrogen gas in the outer space of the metallic bellows within a variable volume cell (B), it is possible to create a saturated-and/or a compressed-liquid condition. The saturated-liquid condition was determined from careful visual observation of the appearance and disappearance of a bubble in the liquid sample.

The experimental apparatus used for the present measurements has originally been constructed by Maezawa et al.¹ and modified by Widiatmo et al.² Since then, we have completed a series of similar measurements with respect to HCFC and HFC refrigerants and their mixtures including R-134a (Maezawa et al.¹), R-123 (Maezawa et al.¹), R-141b (Maezawa et al.³), R-142b (Maezawa et al.⁴), R-22 + R-152a (Maezawa et al.⁵), R-225ca (Widiatmo et al.⁶), R-225cb (Widiatmo et al.⁶), R-22 + R-142b (Maezawa et al.⁷), R-22 + R-152a + R-142b (Maezawa et al.⁷), R-32 (Widiatmo et al.⁸), R-125 (Widiatmo et al.⁸), R-143a (Widiatmo et al.⁹), R-32 + R-134a (Widiatmo et al.¹⁰), R-32 + R-125 (Widiatmo et al.²), R-125 + R-143a (Fujimine et al.¹¹), R-32 + R-134a (Fujimine et al.¹²), R-125 + R-134a (Fujimine et al.¹²), R-32 + R-125 + R-134a (Fujimine et al.¹²) and R-32 + R-125 + R-143a (Widiatmo et al.¹³).

The sample purities, as analyzed by the chemical manufacturer, are 99.99 mass% for $\text{CF}_3\text{CF}_2\text{OCH}_3$ and 99.9 mass% for $\text{CF}_3\text{CF}_2\text{CF}_2\text{OCH}_3$. These samples were provided by the Research Institute of Innovative Technology for the Earth (RITE) Tsukuba, Japan.

We estimated the uncertainties of the present measurements according to the ISO recommendation¹⁴ in terms of the expanded uncertainties with a coverage factor of 2. The experimental uncertainties of temperature, pressure and density measurements were estimated to be within ± 8 mK, ± 2 kPa, and $\pm 2.2 \text{ kg}\cdot\text{m}^{-3}$, respectively.

Results and Discussion

Fifteen vapor pressures and saturated-liquid densities, and 49 compressed-liquid densities of $\text{CF}_3\text{CF}_2\text{OCH}_3$ have been measured at temperatures from 260 to 370 K in 10 K interval and pressures up to 3 MPa. The numerical experimental results are summarized in Table 1, whereas their distribution is illustrated in Figure 2. For $\text{CF}_3\text{CF}_2\text{CF}_2\text{OCH}_3$, 22 vapor pressures and saturated-liquid densities, and 80 compressed-liquid densities have been measured for temperatures 250 - 370 K and pressures up to 3 MPa. The obtained data are tabulated in Table 2 and their distribution is illustrated in Figure 3.

Widiatmo and Watanabe¹⁵ developed the vapor pressure correlations both for $\text{CF}_3\text{CF}_2\text{OCH}_3$ and $\text{CF}_3\text{CF}_2\text{CF}_2\text{OCH}_3$ by using the present data added with the data by Tsuge et al.^{16, 17} and Uchimura et al.¹⁸, in a functional form given in eq 1.

$$\ln P_r = \frac{T_c}{T} (a_1 \tau + a_2 \tau^{1.5} + a_3 \tau^3 + a_4 \tau^6) \quad (1)$$

where P_r and τ is defined as P / P_c and $1 - (T / T_c)$, respectively. The critical temperature, T_c , used in eq 1 for $\text{CF}_3\text{CF}_2\text{OCH}_3$ is that reported by Yoshii et al.¹⁹, while that of $\text{CF}_3\text{CF}_2\text{CF}_2\text{OCH}_3$ by Sako et al.²⁰ The critical pressures, P_c , in eq 1 are those determined by Widiatmo and Watanabe¹⁵ for both compounds. The critical temperatures and pressures are given in Table 3, while coefficients a_1 - a_4 in Table 4.

The vapor pressure deviation of $\text{CF}_3\text{CF}_2\text{OCH}_3$ from eq 1, as illustrated in Figure 4, shows that the present measured vapor pressures agree satisfactorily with the data by Tsuge et al.^{16, 17} within our claimed uncertainty. On the other hand, the vapor pressures calculated from the vapor pressure correlation developed by Sako et al.²⁰ show a significant deviation both from the present data and the data by Tsuge et al.^{16, 17}

This may reflect the existence of systematic error in development of vapor pressure correlation by Sako et al.²⁰

Figure 5 depicts the vapor pressure deviation of CF₃CF₂CF₂OCH₃ from eq 1. As also seen in Figure 4, the vapor pressures calculated from the vapor pressure correlation developed by Sako et al.²⁰ deviate systematically to greater values with increasing temperature. On the contrary, the present vapor pressure and those by Tsuge et al.^{16, 17} are in agreement within ± 2 kPa. From Figures 4 and 5, it can be concluded that those vapor pressure correlations by Sako et al.²⁰ were developed on the basis of less reliable vapor pressure data. Since there is no numerical data available in their reports, detailed discussion about the measurements by Sako et al.²⁰ cannot be done.

For the purpose of data comparison, the saturated-liquid density correlation developed by Widiatmo and Watanabe¹⁵ and given in eq 2 is referred in the present study.

$$\rho' = \rho_c [1 + B(1 - T_r)^\beta + \sum_{i=1}^3 B_i (1 - T_r)^{b_i/3}] \quad (2)$$

The critical density, ρ_c , used in eq 2 for CF₃CF₂OCH₃ is that reported by Yoshii et al.¹⁹, while that for CF₃CF₂CF₂OCH₃ by Sako et al.²⁰. The numerical values of critical densities are given in Table 3, while coefficients B and B₁ through B₃ together with respective exponents are given in Table 4.

Figure 6 illustrates the saturated-liquid density deviation of CF₃CF₂OCH₃ from eq 2. Earlier measurements by Tsuge et al.^{16, 17} are also represented in Figure 6. As shown in Figure 6., the present measurements agree well with the data by Tsuge et al.^{16, 17} Concerning CF₃CF₂CF₂OCH₃, as given in Figure 7, the present measurements also show an excellent agreement with the data by Yoshii et al.¹⁹, and a smooth extension to

those by Uchimura et al.¹⁸

Sato²¹ has successfully developed an empirical equation of state to represent the liquid-phase thermodynamic properties of the compressed water, which is given below;

$$f_1^L = (P_r + D)^C / E \quad (3)$$

where $\rho_r = \rho / \rho_c$, and $P_r = P / P_c$. We have also challenged to apply eq 3 to represent the compressed-liquid densities measured in the present study. The exponent C and coefficients D and E are correlated using functional forms given in eqs 4 through 6.

$$C = c_0 + c_1\tau \quad (4)$$

$$D = d_0 + d_1\tau + d_2\tau^2 + d_3\tau^3 + d_4\tau^4 \quad (5)$$

$$E = e_0 + e_1\tau + e_2\tau^2 + e_3\tau^3 + e_4\tau^4 \quad (6)$$

The numerical constants in eqs 4 - 6 are given in Table 4. The data used to determine the numerical constants in eq 3 include the present saturated- and compressed-liquid densities in the range of 260 – 370 K for $\text{CF}_3\text{CF}_2\text{OCH}_3$, 250 – 370 K for $\text{CF}_3\text{CF}_2\text{CF}_2\text{OCH}_3$, pressures up to 3 MPa and densities 1000 – 1250 $\text{kg}\cdot\text{m}^{-3}$. The liquid density deviation from eq 3 is plotted in Figures 8 and 9 for $\text{CF}_3\text{CF}_2\text{OCH}_3$, and in Figures 10 and 11 for $\text{CF}_3\text{CF}_2\text{CF}_2\text{OCH}_3$, respectively. As shown in those figures, eq 3 represents the present compressed-liquid densities satisfactorily within $\pm 0.2\%$.

It should be noted that the present model, eq 3, provides physically-sound behaviors with respect to essential thermodynamic properties such as specific isochoric and isobaric heat capacities, speed of sound and Joule-Thomson coefficient, by introducing the specific isobaric heat capacity values along the saturated liquid curve as a reference standard. The $P\rho T$ behavior seems acceptable to be extrapolated even to higher pressures up to 10 MPa in the range of temperatures from 230 K to the critical

temperature. Regarding the behaviors of other derived thermodynamic properties mentioned above, however, it is also found that the present model cannot reproduce some acceptable behaviors in the vicinity of the critical point.

Conclusions

Forty-nine compressed-liquid densities, fifteen vapor-pressures and saturated-liquid densities of $\text{CF}_3\text{CF}_2\text{OCH}_3$ have been measured over a range of temperatures 260-370 K and pressures up to 3 MPa. Eighty compressed-liquid densities, twenty-two vapor-pressures and saturated-liquid densities of $\text{CF}_3\text{CF}_2\text{CF}_2\text{OCH}_3$ have also been obtained over a range of temperatures 250-370 K and pressures up to 3 MPa.

Based on the present measurements, a simple thermodynamic model to represent the compressed-liquid densities have also been developed for $\text{CF}_3\text{CF}_2\text{OCH}_3$ and $\text{CF}_3\text{CF}_2\text{CF}_2\text{OCH}_3$, which enabled to reproduce the measured data within ± 0.2 % in density.

Acknowledgements

The present study was partially supported by the New Energy and Industrial Technology Development Organization (NEDO), Tokyo, through the Research Institute of Innovative Technology for the Earth (RITE), Kyoto. The RITE also kindly furnished the sample for the present study. An assistance given by T. Fukabori is greatly acknowledged in the present measurements.

References Cited

- (1) Maezawa, Y.; Sato, H.; Watanabe, K. Saturated liquid densities of HCFC 123 and HFC 134a, *J. Chem. Eng. Data* **1990**, *35*, 225-228.
- (2) Widiatmo, J. V.; Sato, H.; Watanabe, K. Saturated-liquid densities and bubble-point pressures of the binary system HFC-32 + HFC-125, *High Temperatures - High Pressures* **1993**, *25*, 677-683.
- (3) Maezawa, Y.; Sato, H.; Watanabe, K. Liquid densities and vapor pressures• of 1,1,2,2-tetrafluoroethane (HFC-134) and 1,1-dichloro-1-fluoroethane (HCFC-141b), *J. Chem. Eng. Data* **1991**, *36*, 151-155.
- (4) Maezawa, Y.; Sato, H.; Watanabe, K. Liquid densities and vapor pressures of 1-chloro-1, 1-difluoroethane (HCFC 142b), *J. Chem. Eng. Data* **1991**, *36*, 148-150.
- (5) Maezawa, Y.; Sato, H.; Watanabe, K. Saturated liquid densities and bubble-point pressures of binary HCFC 22 + HFC 152a system, *Fluid Phase Equil.* **1991**, *61*, 263-273.
- (6) Widiatmo, J. V.; Maezawa, Y.; Sato, H.; Watanabe, K. Liquid densities and vapor pressure of HCFC 225ca and HCFC 225cb, *Fluid Phase Equil.* **1992**, *80*, 227-238.
- (7) Maezawa, Y.; Widiatmo, J. V.; Sato, H.; Watanabe, K. Saturated liquid densities and bubble point pressures of the ternary HCFC-22+HFC-152a+HCFC-142b system, *Fluid Phase Equil.* **1991**, *67*, 203-212.
- (8) Widiatmo, J. V.; Sato, H.; Watanabe, K. Measurement of vapor pressures and liquid densities of HFC-32 and HFC-125, *Proc. of the 3rd Asian Thermophys. Prop. Conf.* **1992**, 364-369.
- (9) Widiatmo, J. V.; Sato, H.; Watanabe, K. Saturated-liquid densities and vapor pressures of 1, 1, 1 - trifluoroethane, difluoromethane, and pentafluoroethane, *J.*

- Chem. Eng. Data* **1994**, 39, 304-308.
- (10) Widiatmo, J. V.; Sato, H.; Watanabe, K. Measurements of liquid densities of the binary HFC-32 + HFC-134a system, *Fluid Phase Equil.* **1994**, 99, 199-207.
- (11) Fujimie, T.; Sato, H.; Watanabe, K. Bubble-point pressures, saturated and compressed liquid densities of the binary R-125 + HFC-143a system, *Int. J. Thermophys.* **1999**, 20, 911-922.
- (12) Fujimie, T.; Ohta, H.; Sato, H.; Watanabe, K. Liquid densities of alternative refrigerants blended with difluoromethane, pentafluoroethane, and 1,1,1,2-tetrafluoroethane, *J. Chem. Eng. Data* **1997**, 42, 225-228.
- (13) Widiatmo, J. V.; Fujimie, T.; Ohta, H.; Sato, H.; Watanabe, K. Bubble-point pressures and liquid densities of mixtures blended with difluoromethane, pentafluoromethane, and 1,1,1-trifluoromethane, *J. Chem. Eng. Data* **1999**, 44, 1315-1320.
- (14) International Organization for Standardization, Guide to the Expression of Uncertainty in Measurement, Switzerland, **1993**.
- (15) Widiatmo, J. V.; Watanabe, K. Thermodynamic properties of new refrigerants, pentafluoroethyl methyl ether and heptafluoropropyl methyl ether, *Paper to be presented at the 14th Symp. on Thermophys. Prop.* Boulder, Colorado, U.S.A., June 25-30, **2000**.
- (16) Tsuge, T.; Sato, H.; Watanabe, K. Vapor pressures and *PVT* properties of HFE-245mc (pentafluoroethyl methyl ether), *Proc. of Int. Conf. on High Pressure Science and Tech.* 7, Kyoto, Japan, **1998**, 1198-1120.
- (17) Tsuge, T.; Sato, H.; Watanabe, K. Thermodynamic properties and cycle performance of a new alternative refrigerant, HFE-245mc, *Proc. of Int. Conf. on*

Ozone Protection Technologies, Baltimore, U.S.A., **1997**, 17-25.

- (18) Uchimura, A.; Sato, H.; Watanabe, K. Experimental study on the *PVT* properties of new refrigerant $\text{CF}_3\text{CF}_2\text{CF}_2\text{OCH}_3$, *Proc. of the 5th Asian Thermophys. Prop. Conf.*, Seoul, **1998**, 281-284.
- (19) Yoshii, Y.; Mizukawa, M.; Widiatmo, J. V.; Watanabe K., Measurements of saturation densities in critical region of pentafluoroethyl methyl ether (245cbE β), *Paper to be presented at the 14th Symp. on Thermophys. Prop.* Boulder, Colorado, U.S.A., June 25-30, **2000**.
- (20) Sako, T.; Sato, M.; Nakazawa, N.; Oowa, M.; Yasumoto, M.; Ito, H.; Yamashita, S. Measurements of critical properties of fluorinated ethers as alternative refrigerants, *J. Chem. Eng. Data* **1996**, 41, 802-805.
- (21) Sato H. Ph.D. Dissertation, The study of the *PVT* surface of vapor and liquid water under high pressures (in Japanese), Keio University, Yokohama, Japan, **1981**.
- (22) Nakazawa, N.; Sako, T.; Nakane, T.; Sekiya, A.; Kawamura, M.; Sato, M.; Motizuki, Y.; Takada, T.; Yasumoto, M. Liquid densities of fluorinated ethers (in Japanese), *Proc. of 1997 JSRAE Annual Conf.* **1997**, 105-112.

Table 1. Measured P - ρ - T Properties for $\text{CF}_3\text{CF}_2\text{OCH}_3$

T / K	P / kPa	$\rho / (\text{kg}\cdot\text{m}^{-3})$	T / K	P / kPa	$\rho / (\text{kg}\cdot\text{m}^{-3})$
259.984	43.5	1373.8 *	319.986	2499.1	1210.7
			319.986	3001.6	1213.7
269.986	69.0	1347.7 *			
269.986	69.0	1346.3 *	329.985	535.1	1163.0 *
			329.985	997.0	1167.1
279.989	104.8	1319.5 *	329.985	1496.8	1170.9
279.989	104.7	1319.1 *	329.985	1993.8	1174.7
279.989	502.4	1320.5	329.985	2503.2	1178.7
279.989	1003.9	1322.5	329.985	3005.5	1182.4
279.989	1501.8	1324.4			
279.989	1998.7	1326.3	339.985	694.9	1126.2 *
279.989	2504.2	1328.3	339.985	1007.3	1129.6
279.989	3007.4	1330.0	339.985	1498.9	1134.3
			339.985	1999.3	1139.2
289.988	153.3	1290.9 *	339.985	2501.2	1143.6
289.988	504.7	1292.3	339.985	2994.4	1148.3
289.988	996.1	1294.6			
289.988	1496.4	1296.8	349.984	888.0	1086.4 *
289.988	1996.3	1299.0	349.984	1494.3	1094.3
289.988	2503.8	1300.9	349.984	1999.3	1100.3
289.988	2997.7	1303.0	349.984	2496.3	1105.8
			349.984	2998.4	1111.2
299.987	217.3	1260.8 *			
299.987	218.2	1260.9 *	359.984	1119.0	1042.4 *
299.987	501.2	1262.4	359.984	1502.0	1048.8
299.987	1001.5	1264.9	359.984	1997.0	1056.8
299.987	1501.1	1267.3	359.984	2500.0	1064.0
299.987	2000.5	1269.5	359.984	2996.3	1070.9
299.987	2501.2	1272.2			
299.987	2998.4	1274.2	369.983	1393.0	992.9 *
			369.983	1993.2	1006.5
309.986	300.1	1229.8 *	369.983	2498.6	1016.4
309.986	999.8	1233.7	369.983	2996.4	1025.5
309.986	1498.7	1236.7			
309.986	2000.1	1239.6	*Observed values at two phase condition.		
309.986	2501.9	1242.3			
309.986	2998.2	1244.7			
319.986	404.5	1196.6 *			
319.986	1006.4	1201.0			
319.986	1502.3	1205.9			
319.986	2002.1	1207.7			

Table 2. Measured P - ρ - T Properties for $\text{CF}_3\text{CF}_2\text{CF}_2\text{OCH}_3$

T / K	P / kPa	$\rho / (\text{kg}\cdot\text{m}^{-3})$	T / K	P / kPa	$\rho / (\text{kg}\cdot\text{m}^{-3})$
249.981	4.8	1528.3 *	319.986	155.8	1341.2 *
			319.986	746.8	1344.1
259.984	10.2	1504.0 *	319.986	1001.3	1345.4
			319.986	1503.0	1347.8
269.986	18.9	1478.9 *	319.986	2084.5	1351.2
			319.986	2450.5	1353.0
279.989	31.7	1452.7 *	319.986	2993.6	1355.6
279.988	31.5	1452.9 *			
279.988	500.4	1454.3	329.985	214.6	1311.7 *
279.988	1005.3	1456.0	329.985	213.8	1311.5 *
279.988	1506.5	1457.9	329.985	213.9	1312.4 *
279.988	2003.5	1459.5	329.985	503.4	1313.3
279.988	2499.6	1461.2	329.985	999.6	1316.4
279.988	3004.2	1462.6	329.985	1497.8	1319.3
			329.985	1999.1	1322.3
289.989	49.8	1425.8 *	329.985	2499.9	1325.4
289.989	550.1	1428.7			
289.989	1011.5	1429.9	329.985	2995.6	1327.9
289.989	1502.9	1432.2	329.985	504.5	1314.7
289.989	2007.0	1433.6	329.985	998.8	1317.4
289.989	2504.8	1435.5	329.985	1500.2	1320.3
289.989	2998.9	1437.2	329.985	2010.3	1323.7
			329.985	2505.8	1327.0
299.987	75.5	1399.6 *	329.985	2989.8	1329.0
299.987	534.7	1400.4			
299.987	996.3	1403.3	339.985	288.7	1281.0 *
299.987	1504.4	1404.6	339.985	288.1	1280.6 *
299.987	2007.0	1407.0	339.985	288.2	1280.6 *
299.987	2499.9	1408.6	339.985	508.3	1281.9
299.987	2992.0	1410.3	339.985	1002.7	1285.5
			339.985	1503.7	1288.9
309.986	110.2	1370.5 *	339.985	2000.1	1292.4
309.986	557.3	1372.3	339.985	2503.7	1295.7
309.986	1008.3	1374.1	339.985	3000.6	1298.9
309.986	1501.4	1376.8	339.985	522.7	1282.3
309.986	2000.3	1379.7	339.985	998.4	1285.7
309.986	2502.3	1381.6	339.985	1493.5	1288.9
309.986	2992.0	1383.6	339.985	2007.9	1292.5
			339.985	2505.4	1296.0
			339.985	3006.3	1299.2

Table 2. (continued)

T / K	P / kPa	$\rho / (\text{kg}\cdot\text{m}^{-3})$
349.985	381.9	1247.8*
349.985	380.4	1247.2*
349.985	380.7	1246.2*
349.985	501.8	1248.2
349.985	1000.6	1252.4
349.985	1502.5	1256.4
349.985	2009.8	1260.4
349.985	2500.6	1264.2
349.985	2998.5	1268.7
349.985	998.3	1251.4
349.985	1504.6	1255.8
349.985	2001.2	1259.3
349.985	2507.7	1263.5
349.985	2998.2	1267.1

T / K	P / kPa	$\rho / (\text{kg}\cdot\text{m}^{-3})$
359.984	494.7	1211.4*
359.984	493.7	1212.1*
359.984	493.9	1210.6*
359.984	1010.0	1217.3
359.984	1505.6	1222.2
359.984	2002.4	1226.7
359.984	2506.1	1231.2
359.984	2996.1	1235.2
359.984	1000.9	1215.6
359.984	1505.3	1220.8
359.984	2001.7	1225.7
359.984	2507.6	1230.4
359.984	3002.6	1234.3
369.983	631.3	1173.6*
369.983	1003.2	1178.2
369.983	1498.7	1183.9
369.983	2004.0	1189.9
369.983	2501.7	1194.9
369.983	2993.0	1200.2

*Observed values at two phase condition.

Table 3. Critical Parameters for $\text{CF}_3\text{CF}_2\text{OCH}_3$ and $\text{CF}_3\text{CF}_2\text{CF}_2\text{OCH}_3$

	$\text{CF}_3\text{CF}_2\text{OCH}_3$	$\text{CF}_3\text{CF}_2\text{CF}_2\text{OCH}_3$
P_c / MPa	2.887 ^a	2.476 ^b
T_c / K	406.83 ^a	437.7 ^c
$\rho_c / (\text{kg}\cdot\text{m}^{-3})$	509 ^a	530 ^c

^a Yoshii et al.¹⁹, ^b Uchimura et al.¹⁸, ^c Sako et al.²⁰

Table 4. Coefficients in eqs 1 – 3 for $\text{CF}_3\text{CF}_2\text{OCH}_3$ and $\text{CF}_3\text{CF}_2\text{CF}_2\text{OCH}_3$

	$\text{CF}_3\text{CF}_2\text{OCH}_3$	$\text{CF}_3\text{CF}_2\text{CF}_2\text{OCH}_3$
a_1	-7.73986	-7.95132
a_2	1.52151	1.50989
a_3	-4.05631	-4.48124
a_4	-11.0921	-20.8350
B	1.43926	1.81014
B_1	1.69075	0.98763
B_2	-1.54018	-
B_3	1.57395	-
B	0.322	0.325
b_1	2	2.36
b_2	4	-
b_3	6	-
c_0	0.084716	0.074730
c_1	-0.17288	-0.11568
d_0	-0.99575	-0.99907
d_1	12.306	11.368
d_2	69.742	106.35
d_3	-359.41	-456.44
d_4	545.71	570.32
e_0	0.56963	0.56658
e_1	-0.69563	-0.71530
e_2	0.49193	0.73236
e_3	0.28421	-0.43312
e_4	-0.71301	0.098989

Figure Captions

Figure 1. Experimental Apparatus: (A), magnetic densimeter; (B), variable volume cell; (C), digital quartz pressure transducer; (D), damper; (E), thermostated fluid bath; (F), digital quartz pressure gauge; (G), vacuum pump; (H), vacuum gauge; (I), nitrogen gas; (J), digital quartz pressure computer; (K), main heater; (L), subheater; (M), cooler; (N), stirrer; (O), standard resistor; (P), PID controller; (R), standard platinum resistance thermometer; (S), pressure gauge; (T), digital multimeter; (U), current controller; (V1-10), valves; (W), DC power supply; (X), galvanometer; (Y), thermometer bridge; (Z), pen recorder; (Ω), transformer; (Φ), personal computer

Figure 2. Present experimental data for $\text{CF}_3\text{CF}_2\text{OCH}_3$ on P - ρ - T surface:

Saturated-liquid densities: \bullet , Data on P - ρ - T diagram; $-$, Saturation curve;

Compressed-liquid densities: \circ , Data on P - ρ - T diagram

Figure 3. Present experimental data for $\text{CF}_3\text{CF}_2\text{CF}_2\text{OCH}_3$ on P - ρ - T surface:

Saturated-liquid densities: \bullet , Data on P - ρ - T diagram; $-$, Saturation curve

Compressed-liquid densities: \circ , Data on P - ρ - T diagram

Figure 4. Vapor-pressure deviation for $\text{CF}_3\text{CF}_2\text{OCH}_3$: \bullet , This work; Δ , Tsuge et al.^{16, 17}; $-$, Sako et al.²⁰

Figure 5. Vapor-pressure deviation for $\text{CF}_3\text{CF}_2\text{CF}_2\text{OCH}_3$: \bullet , This work; \times , Uchimura et al.¹⁸; $-$, Sako et al.²⁰

Figure 6. Saturated-liquid density deviation for $\text{CF}_3\text{CF}_2\text{OCH}_3$: \bullet , This work; Δ , Tsuge et al.^{16, 17}

Figure 7. Saturated-liquid density deviation for $\text{CF}_3\text{CF}_2\text{CF}_2\text{OCH}_3$: \circ , This work; \times , Uchimura et al.¹⁸; \square , Nakazawa et al.²²

Figure 8. Liquid-density deviation for $\text{CF}_3\text{CF}_2\text{OCH}_3$ at different temperatures: This work: \bullet , Saturated- liquid densities; \circ , Compressed- liquid densities; Δ , Tsuge et al.^{16, 17}

Figure 9. Liquid-density deviation for $\text{CF}_3\text{CF}_2\text{OCH}_3$ at different pressures: This work: \bullet , Saturated- liquid densities; \circ , Compressed- liquid densities; Δ , Tsuge et al.^{16, 17}

Figure 10. Liquid-density deviation for $\text{CF}_3\text{CF}_2\text{CF}_2\text{OCH}_3$ at different temperatures: This work: \bullet , Saturated- liquid densities; \circ , Compressed- liquid densities; \times , Uchimura et al.¹⁸; \square , Nakazawa et al.²²

Figure 11. Liquid-density deviation for $\text{CF}_3\text{CF}_2\text{CF}_2\text{OCH}_3$ at different pressures: This work: ●, Saturated- liquid densities; ○, Compressed- liquid densities; ×, Uchimura et al.¹⁸; □, Nakazawa et al.²²

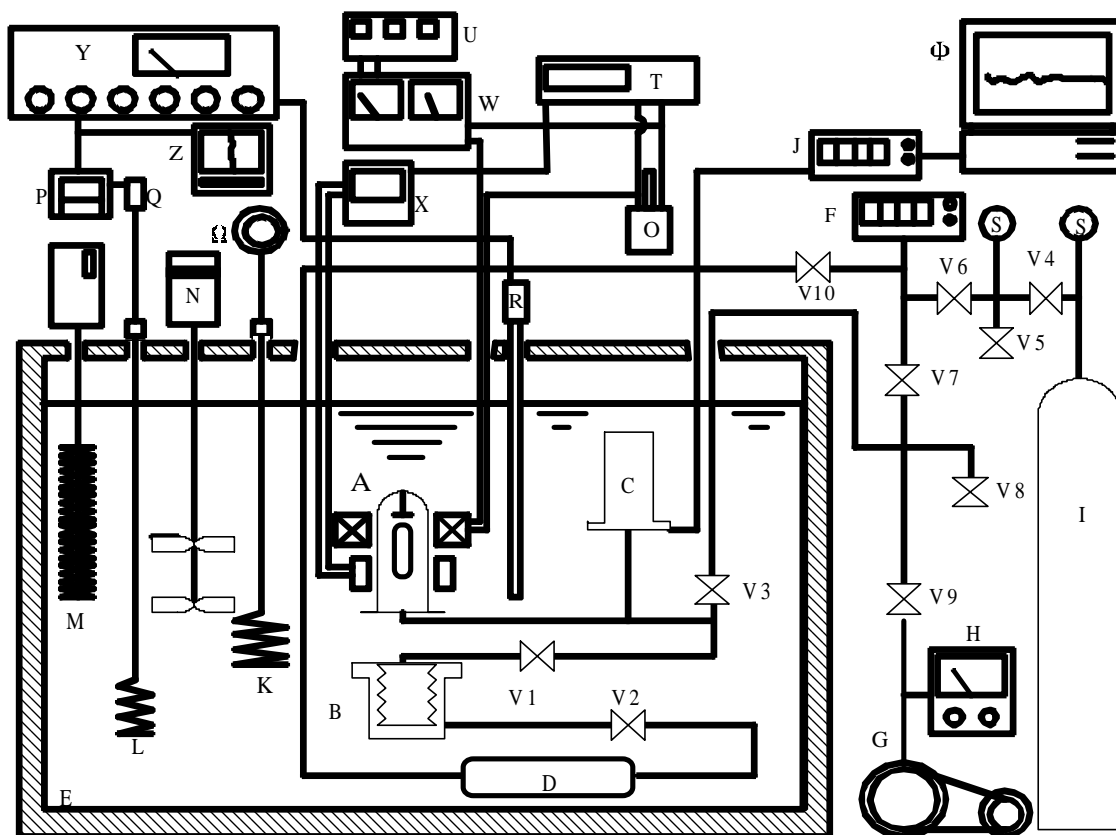


Figure 1. Experimental Apparatus: (A), magnetic densimeter; (B), variable volume cell; (C), digital quartz pressure transducer; (D), damper; (E), thermostated fluid bath; (F), digital quartz pressure gauge; (G), vacuum pump; (H), vacuum gauge; (I) nitrogen gas; (J), digital quartz pressure computer; (K), main heater; (L), subheater; (M), cooler; (N), stirrer; (O), standard resistor; (P), PID controller; (R), standard platinum resistance thermometer; (S), pressure gauge; (T), digital multimeter; (U), current controller; (V 1-10), valves; (W), DC power supply; (X), galvanometer; (Y), thermometer bridge; (Z), pen recorder; (J), transformer; (J), personal computer

Ohta et al.

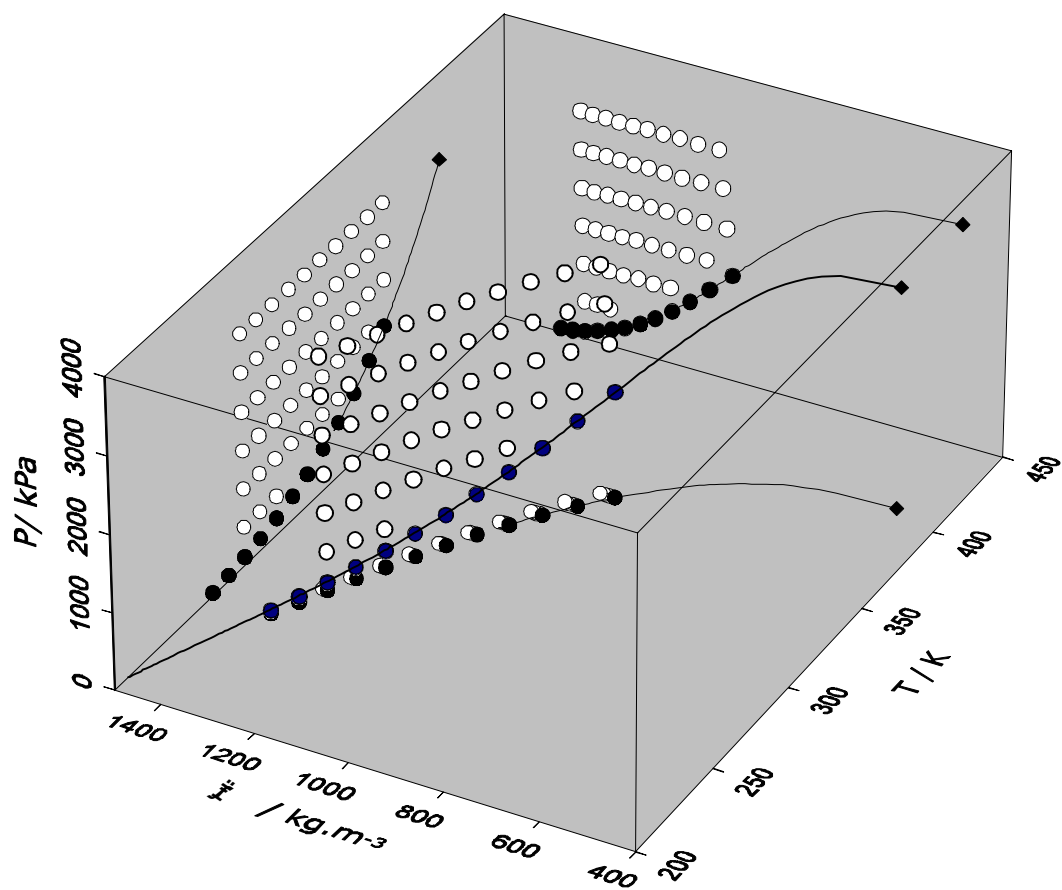


Figure 2. Present experimental data for $\text{CF}_3\text{CF}_2\text{OCH}_3$ on P - ρ - T surface:
 Saturated-liquid densities: \circ , Data on P - ρ - T diagram; \bullet , Saturation curve;
 Compressed-liquid densities: \bullet , Data on P - ρ - T diagram

Ohta et al.

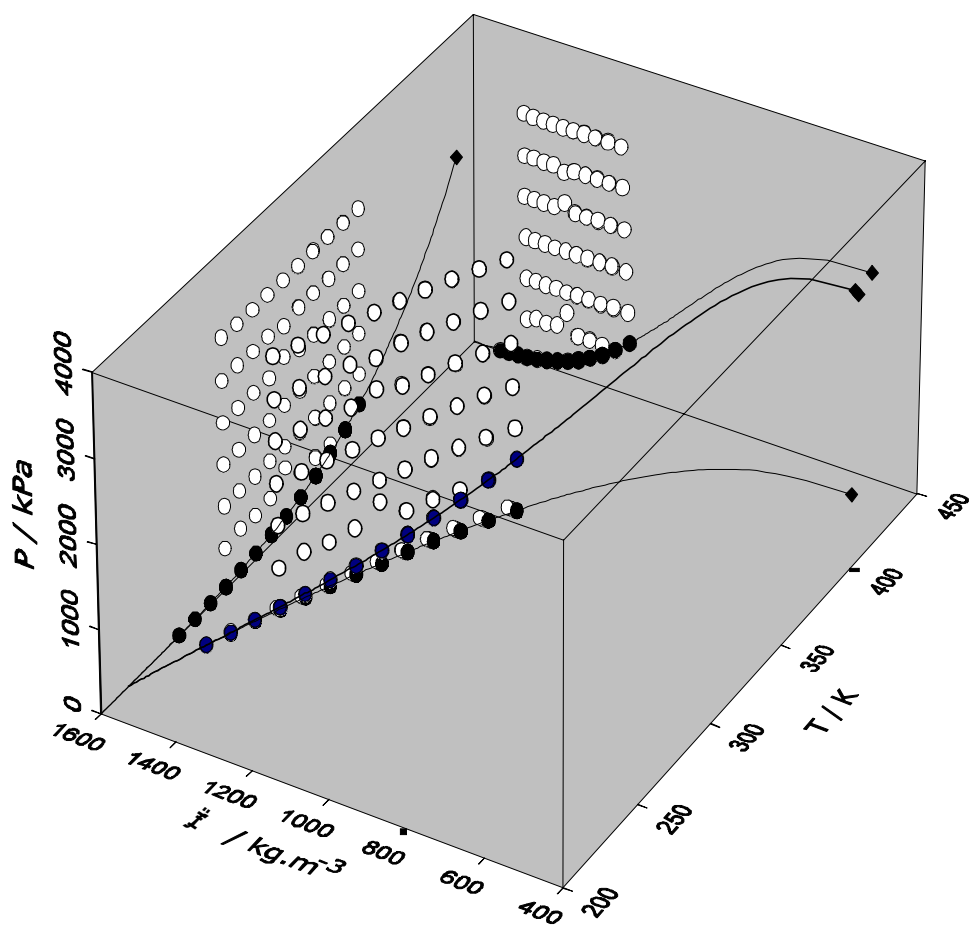


Figure 3. Present experimental data for $\text{CF}_3\text{CF}_2\text{CF}_2\text{OCH}_3$ on P - ρ - T surface:
 Saturated-liquid densities: \circ , Data on P - ρ - T diagram; \bullet , Saturation curve
 Compressed-liquid densities: \bullet , Data on P - ρ - T diagram

Ohta et al.

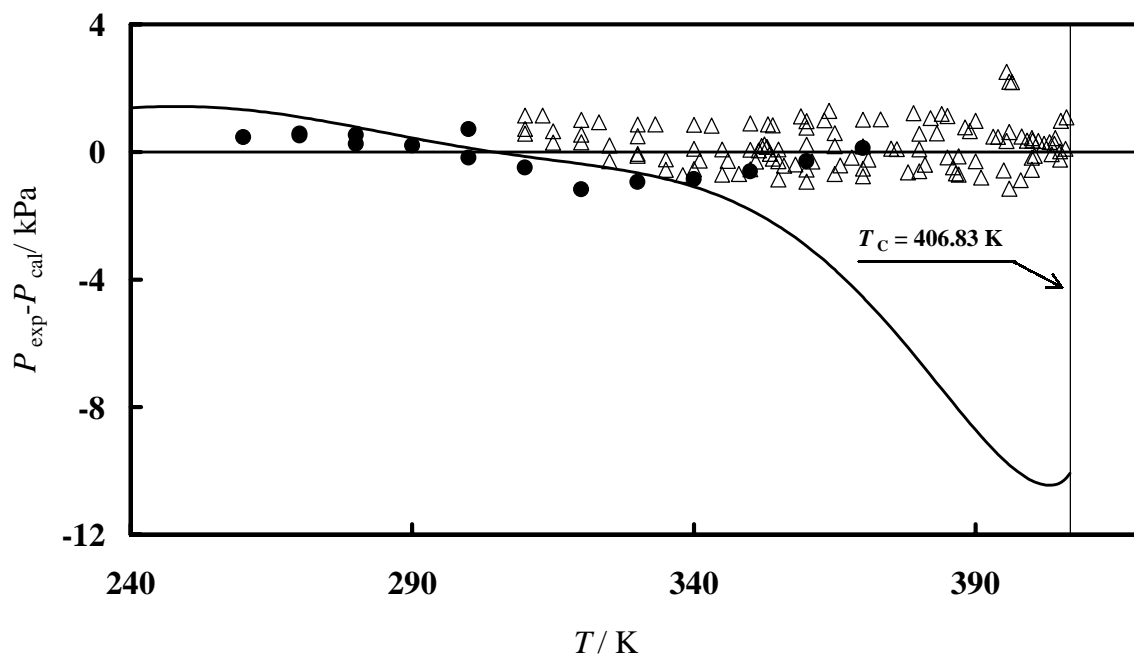


Figure 4. . Vapor-pressure deviation for $\text{CF}_3\text{CF}_2\text{OCH}_3$: ●, This work; Δ, Tsuge et al.^{16, 17}; —, Sako et al.²⁰

Ohta et al.

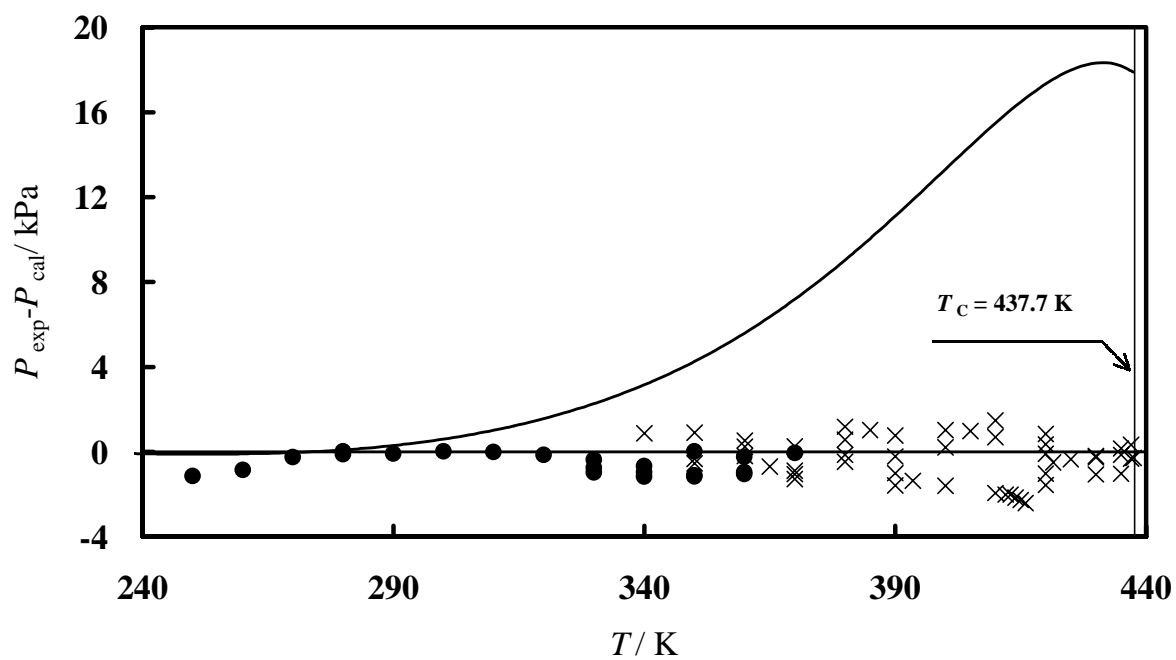


Figure 5. Vapor-pressure deviation for $\text{CF}_3\text{CF}_2\text{CF}_2\text{OCH}_3$: ●, This work; ×, Uchimura et al.¹⁸; —, Sako et al.²⁰

Ohta et al.

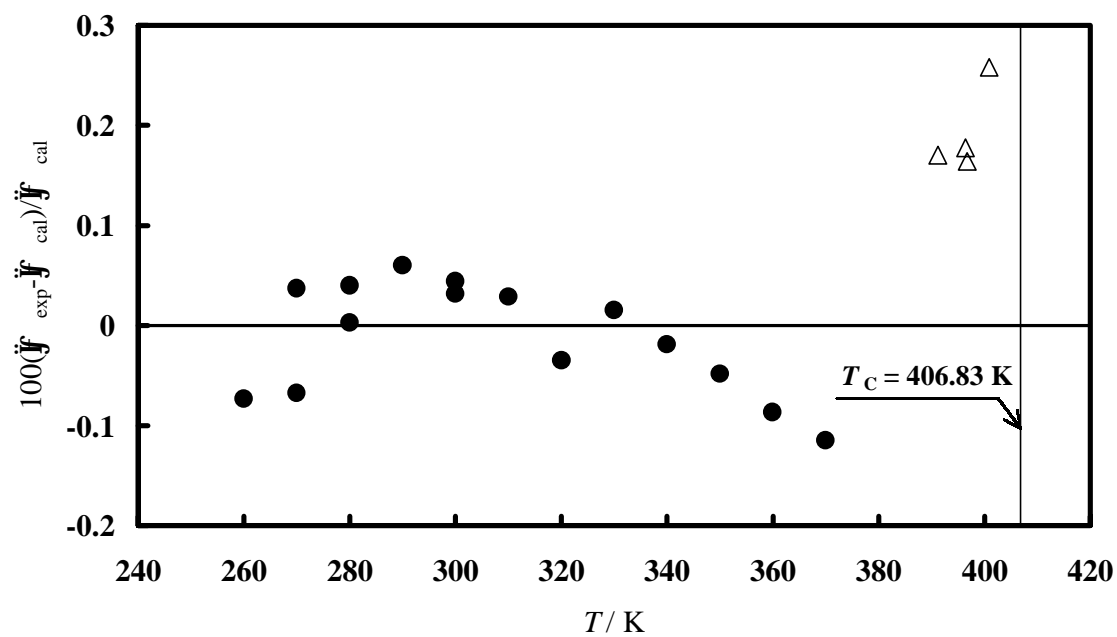


Figure 6. Saturated-liquid density deviation for $\text{CF}_3\text{CF}_2\text{OCH}_3$: ●, This work; Δ, Tsuge et al.^{16, 17}

Ohta et al.

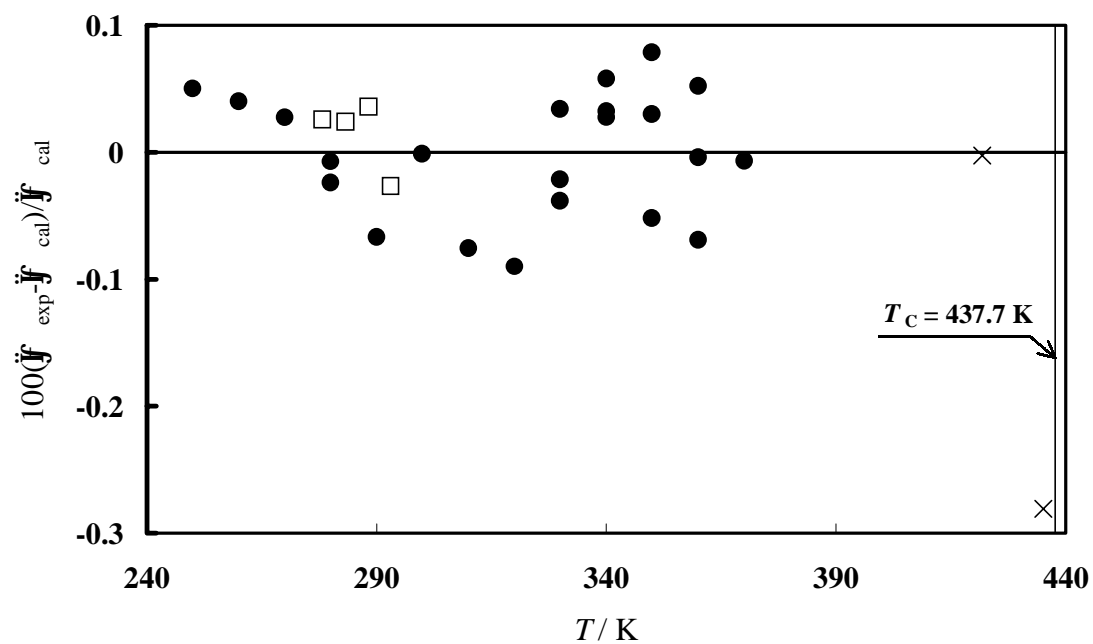


Figure 7. Saturated-liquid density deviation for $\text{CF}_3\text{CF}_2\text{CF}_2\text{OCH}_3$: ○, This work; ×, Uchimura et al.¹⁸; □, Nakazawa et al.²² ◇, Ohta et al.

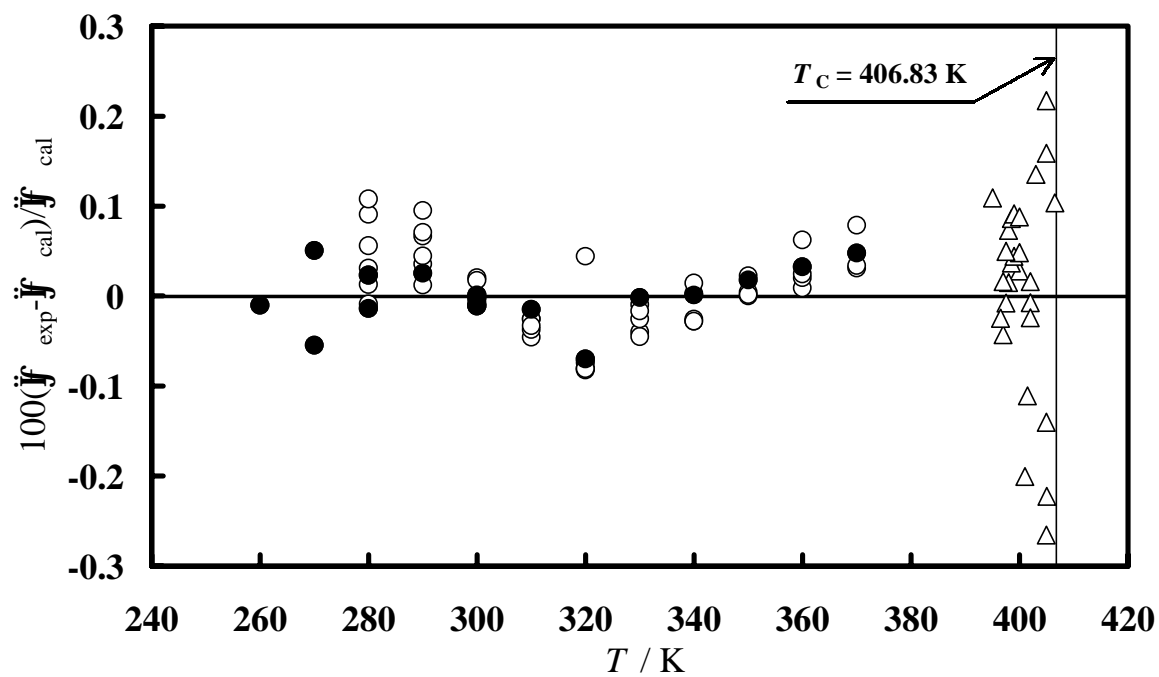


Figure 8. Liquid-density deviation for $\text{CF}_3\text{CF}_2\text{OCH}_3$ at different temperatures: This work: ●, Saturated- liquid densities; ○, Compressed- liquid densities; Δ, Tsuge et al.¹⁶,
17

Ohta et al.

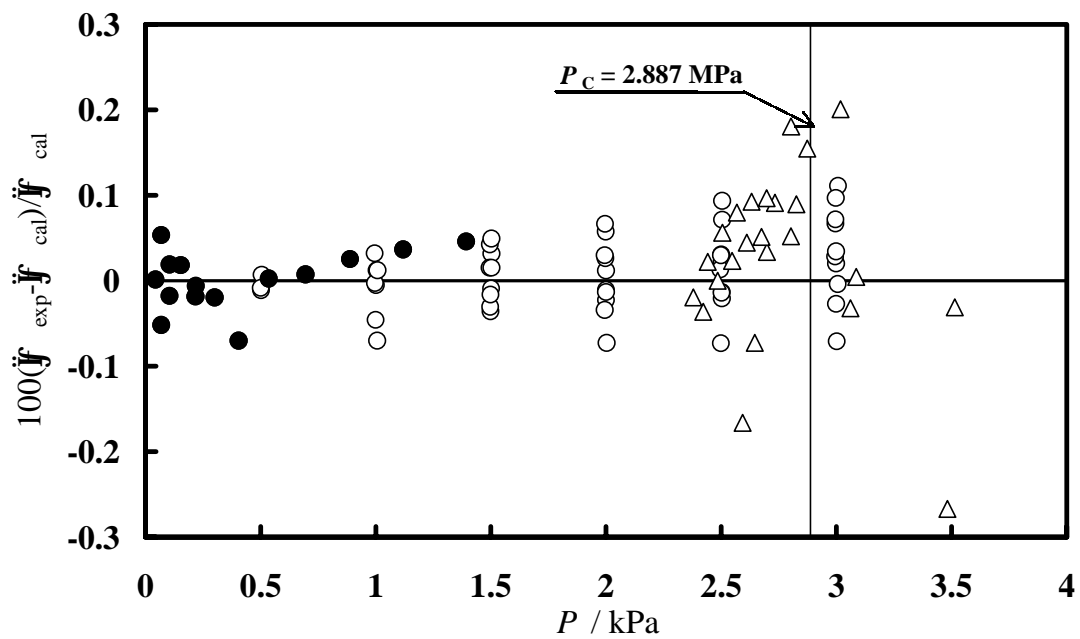


Figure 9. Liquid-density deviation for $\text{CF}_3\text{CF}_2\text{OCH}_3$ at different pressures: This work:

●, Saturated- liquid densities; ○, Compressed- liquid densities; Δ, Tsuge et al.^{16, 17}

Ohta et al.

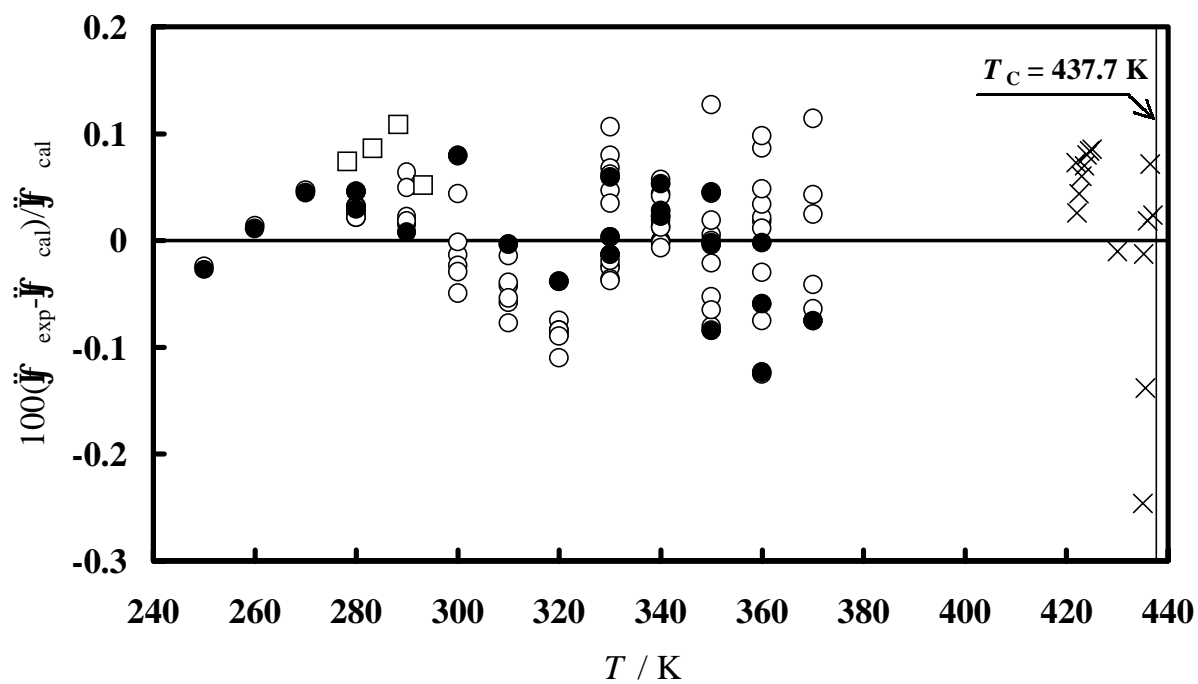


Figure 10. Liquid-density deviation for $\text{CF}_3\text{CF}_2\text{CF}_2\text{OCH}_3$ at different temperatures: This work: ●, Saturated- liquid densities; ○, Compressed- liquid densities; ×, Uchimura et al.¹⁸; □, Nakazawa et al.²²

Ohta et al.

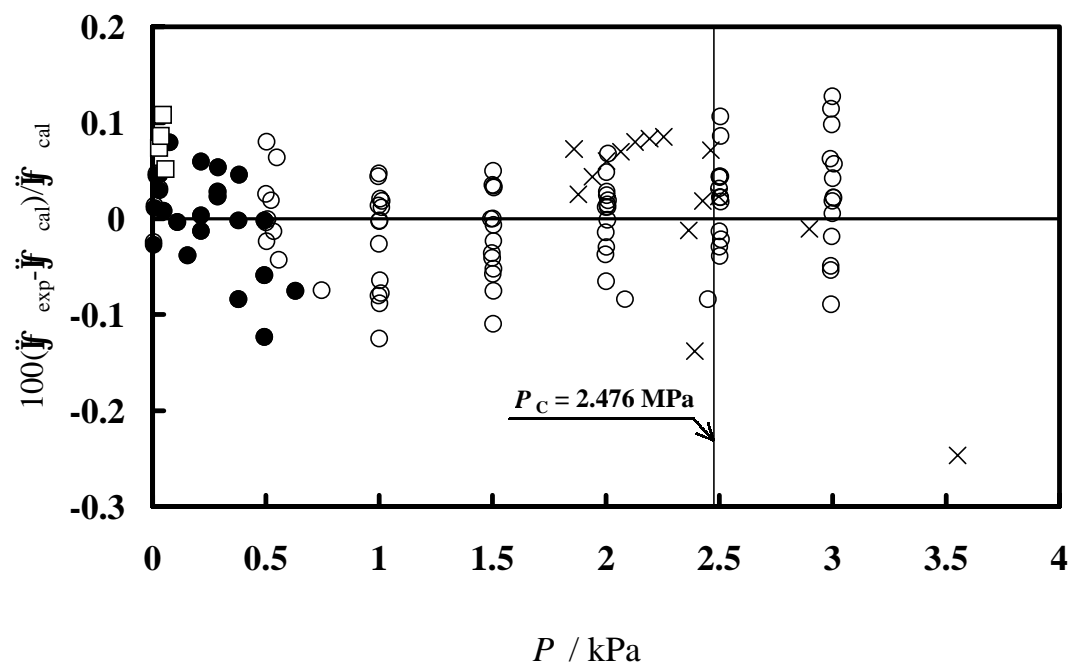


Figure 11 Liquid-density deviation for $\text{CF}_3\text{CF}_2\text{CF}_2\text{OCH}_3$ at different pressures: This work: ●, Saturated- liquid densities; ○, Compressed- liquid densities; ×, Uchimura et al.¹⁸; □, Nakazawa et al.²²

Ohta et al.